Energy Proceedings
Vol 47, 2024
ISSN 2004-2965

Thermo-kinetic Evaluation of Solar Thermochemical Cycle for Hydrogen Production Driven by Carbonaceous Agents#

Tong Liu[1], Jiateng Zhang[1], Ji Li[1], Xiangnan Tang[1], Hui Kong[1, 2*]

1 School of Mechanical Engineering, Beijing Institute of Technology, Beijing 100081, China

2 State Key Laboratory of Power System Operation and Control, Department of Thermal Engineering, Tsinghua-BP Clean Energy Center, Tsinghua University, Beijing 100084, China
*Corresponding author: Hui Kong
(Corresponding Author: *konghui2020@bit.edu.cn*)

ABSTRACT

Solar thermochemical cycling, in which concentrated solar energy is used to split water and produce hydrogen, is considered a promising way to produce green hydrogen in the future. Nonetheless, it encounters issues, including elevated reaction temperatures and significant deoxygenation losses. Here, we propose a high-efficiency solar thermochemical cycling system for hydrogen production driven by carbonaceous agents and establish a thermo-kinetic model for isothermal pressure-swing cycles. Carbon monoxide is introduced as a reducing agent into the reduction reaction, decreasing the Gibbs free energy of oxygen vacancies generated by metal oxygen carriers to lower the reduction temperature while consuming oxygen to create an extremely low oxygen partial pressure environment. This system avoids the problem of large energy losses in traditional deoxygenation methods such as inert sweeping gases and vacuum pumps; moreover, it achieves a synergistic decrease in the reaction temperature and oxygen partial pressure during the thermochemical cycle. The theoretical solar energy to fuel conversion efficiencies of this system under isothermal cycling at 1300 °C can reach 19.89% and 23.77% with only water heat recovery when $CeO_{2-\delta}$ and $Ce_{0.80}Zr_{0.20}O_{2-\delta}$ are used as oxygen carriers, respectively. This research contributes a fresh idea to the problem of the high reaction temperatures and large irreversible losses in the solar thermochemical cycle for hydrogen production.

Keywords: solar thermochemical cycle, hydrogen production, carbonaceous agents, thermo-kinetic model, thermodynamic efficiency

NONMENCLATURE

Symbols	
δ	oxygen non-stoichiometry
$\frac{\mathrm{d}\delta}{\mathrm{d}t}$	rate of change in oxygen non-stoichiometry (min^{-1})
P_{O_2}	oxygen partial pressure (atm)
P_{tot}	total pressure (atm)
ΔH_{red}	change in enthalpy of reduction (kJ mol^{-1})
ΔS_{red}	change in entropy of reduction (J mol^{-1} K^{-1})
F	volume flow rate at the inlet (sccm min^{-1})
χ	volume ratio of the inlet gas
ξ_{CO}	volume ratio of carbon monoxide to carbon dioxide in the inlet gas
ψ_{CO}	extent of reaction of carbon monoxide
ψ_{H_2O}	extent of reaction of water
K_{T_0}	reaction equilibrium constant
n_{CeO_2}	moles of ceria (mol)
M_{CeO_2}	molar mass of ceria (g mol^{-1})
V_M	molar volume (L mol^{-1})
$\dot{V}_{CO}$	cycle-averaged volumetric carbon monoxide consumption rate per gram of oxide (sccm g^{-1})
$\dot{V}_{H_2}$	cycle-averaged volumetric hydrogen production rate per gram of oxide (sccm g^{-1})
$\eta_{solar\text{-}to\text{-}fuel}$	solar energy to fuel conversion efficiency
HHV_{H_2}	higher heating value of hydrogen (kJ mol^{-1})
η_{abs}	absorption efficiency of solar energy

This is a paper for the 10th Applied Energy Symposium: Low Carbon Cities & Urban Energy Systems (CUE2024), May. 11-12, 2024, Shenzhen, China.

Q_{solar}	total solar energy input to the system (kJ)
Q_{red}	energy used for the reduction of oxides (kJ)
Q_{H_2O}	energy used for heating water (kJ)
Q_{CO}	energy used for heating carbon monoxide (kJ)
I	solar irradiation (W m^{-2})
C	concentration ratio
X	conversion rate of reactants
ΔH_{oxide}	molar enthalpy change of ceria (kJ mol^{-1})
$\Delta H^{373K}_{H_2O(l)\rightarrow(g)}$	molar enthalpy change of water from liquid to gas (kJ mol^{-1})
C_p	specific heat capacity (J kg^{-1} K^{-1})

1. INTRODUCTION

To achieve the goal of "carbon neutrality," carbon emissions are closely related to economic development, and the reserves of renewable energy, such as solar energy, are enormous and inexhaustible. Effectively storing or transforming these energy sources into stable energy is an important direction for alleviating energy problems[1]. Hydrogen, as one of the globally recognized clean secondary energy sources, is listed as an important approach to achieve decarbonization[2].

Two-step solar thermochemical cycling is a promising way for utilizing solar energy to produce H_2 and CO, which can be further synthesized into liquid fuels via Fischer-Tropsch reactions, increasing the ease of storage and transportation[3, 4]. This process achieves continuous fuel production through alternating redox reactions of oxygen carriers (usually metal oxides), and significant progress has been made in theoretical and experimental research after decades of effort[5]. Chueh et al. pointed out that the theoretical solar energy to fuel conversion efficiency based on ceria is relatively high, reaching 16-19% even without heat recovery[6]. However, the experimental efficiency is approximately 5-10%, which is much lower than the theoretical efficiency[6, 7]. Marxer et al. conducted consecutive and stable cycles of ceria at reduction temperature of 1500 °C, during which the average solar energy to fuel conversion efficiency was only 5.25% without heat recovery[8]. The main causes of this phenomenon are irreversible losses, such as high-temperature thermal radiation and deoxygenation energy consumption. Researchers have attempted to introduce carbonaceous agents, such as methane[9-11] and solid carbon[12, 13], to assist in the reduction reaction. However, improper input of methane and solid carbon, or excessively high temperatures, will result in carbon deposits on the surface of oxides, which is one of the main reasons why the redox ability of oxygen carriers is disrupted[10, 14-16].

Industrial waste gas often contains a certain number of monocarbon combustibles (CO and CH_4), which are difficult to separate and have a low heating efficiency[17]. Using it as the reducing gas to drive the solar thermochemical cycle is a potential utilization approach. Here, carbon monoxide is simulated as the industrial waste gas input into the cycle to assist in the reduction of oxides, as shown in Figure 1.

However, to our best knowledge, there is almost little theoretical research on the process of the solar thermochemical cycle driven by carbon monoxide. Therefore, a thermal-kinetic model of the solar thermochemical cycling system for hydrogen production driven by carbon monoxide is established and its thermodynamic efficiency is evaluated.

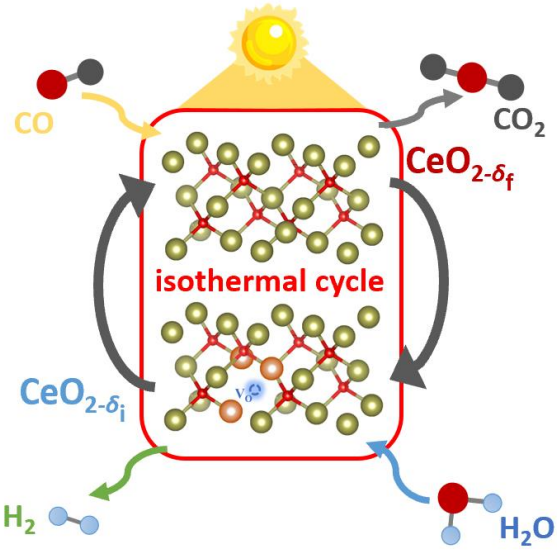

Fig. 1 Schematic diagram of the solar thermochemical cycling system for hydrogen production driven by CO.

2. THERMO-KINETIC MODEL

2.1 Introduction of the system

In this system, the metal oxygen carriers undergo a reduction reaction driven by carbon monoxide, with a reaction temperature range of 1300-1800 °C. Subsequently, under isothermal conditions, a re-oxidation reaction occurs to split water to produce hydrogen. Compared with the dual temperature cycle driven by the temperature gradient, the isothermal cycle is driven by the pressure gradient, avoiding frequently

repeated heating and cooling of the oxygen carriers[18]. A schematic diagram of the system is shown in Figure 2. In addition to pure ceria, $Ce_{0.80}Zr_{0.20}O_{2-\delta}$ doped with 20% zirconium ions was selected as the metal oxygen carrier[19]. The oxygen exchange capacity and anti-sintering resistance of pure ceria are enhanced by doping non-redox zirconium ions[19, 20]. The continuous production of fuel is achieved through the thermochemical cycles of oxygen carriers.

Moreover, it is assumed that the sample of oxygen carriers is sufficiently small and has a specially high internal gas diffusion rate and surface reaction rate. Therefore, oxides will instantly release oxygen until the thermodynamic limitation for forming oxygen vacancies under the programmed airflow and temperature conditions. The oxygen content in the oxides will be fixed by the rate at which the gas is supplied or removed from the surrounding area of the materials when the material dynamics are infinitely fast[21]. Hence, the efficiency of the adopted deoxygenation method has a significant impact on the production capacity of the oxides. Based on this assumption, numerical calculations can be performed on the stoichiometric changes in oxides and gas evolution, thereby predicting the fuel production capacity of the cycles, which has been proven feasible in the research of Haile et al[21, 22].

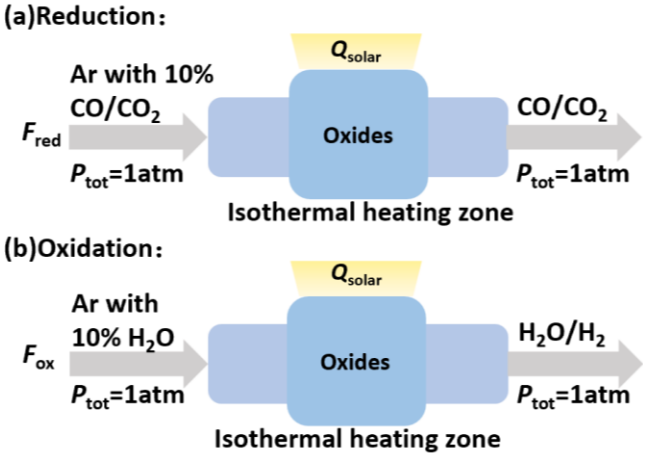

Fig. 2 Schematic diagram of the solar thermochemical cycle under different gas conditions: (a) reduction, and (b) oxidation.

2.2 Model of the reduction step

In the reduction reaction, argon gas (Ar) containing a certain proportion of CO/CO_2 is introduced to simulate industrial waste gas with reducing ability. Oxygen in the surrounding area of the materials is quickly consumed to promote the generation of oxygen vacancies, which is represented by the oxygen non-stoichiometry δ. The reaction formula is:

$$\frac{1}{\Delta\delta}\mathrm{CeO}_{2-\delta_i}+\mathrm{CO}\rightarrow\frac{1}{\Delta\delta}\mathrm{CeO}_{2-\delta_f}+\mathrm{CO}_2 \qquad (1)$$

where $\Delta\delta=\delta_f-\delta_i$, is the variation in the number of oxygen vacancies. Additionally, CO_2 in the airflow decomposes at high temperatures (reaction equation 2), and the degree of this reversible reaction is limited by a temperature-dependent equilibrium constant K_{CO_2,T_0}.

$$\mathrm{CO}_2\rightleftharpoons\mathrm{CO}+\frac{1}{2}\mathrm{O}_2 \qquad (2)$$

At any moment *t*, the oxygen partial pressure of the equilibrium gas around the materials ($P_{O_2}(\delta,T_0)$) is related to the oxygen non-stoichiometry and temperature. If the thermodynamics of the material in reduction reaction, i.e., the enthalpy and entropy represented in equation (1) ($\Delta H_{red}(\delta)$ and $\Delta S_{red}(\delta)$, respectively) are determined, it can be calculated using the following equation:

$$\ln(P_{O_2}(\delta,T))=\frac{-\Delta H_{red}(\delta)+T\Delta S_{red}(\delta)}{RT} \qquad (3)$$

According to the mass balance of the gas in the reduction reaction, the rate of oxygen vacancies over time during the reduction process ($\Delta\delta_{red}=\delta_f-\delta_i$) is obtained:

$$\frac{\mathrm{d}\delta_{red}}{\mathrm{d}t}=\frac{F_{red}}{n_{CeO_2}}\times\frac{(2P_{O_2}(\delta,T_0)+\psi_{CO}\chi_{CO}(P_{tot}-P_{O_2}(\delta,T_0)))}{(P_{tot}-P_{O_2}(\delta,T_0))} \qquad (4)$$

in which F_{red} is the volume flow rate at the inlet during reduction. χ_{CO_x} is the volume fraction of CO and CO_2 contained in the inlet airflow, while ξ_{CO} is the ratio of their volume fractions ($\xi_{CO}=\chi_{CO}/\chi_{CO_2}$). P_{tot} is the total pressure during the cycles, set at 1 atm. ψ_{CO} is the proportion of CO that undergoes oxidation, and it has the following relationship with K_{CO_2,T_0}:

$$K_{CO_2,T_0}=\frac{(1-\psi_{CO})\xi_{CO}}{1+\psi_{CO}\xi_{CO}}P_{O_2}(\delta,T_0)^{\frac{1}{2}} \qquad (5)$$

Due to the extremely low oxygen partial pressure (less than 10^{-5} atm) during the reduction process, the unremoved oxygen is ignored when calculating the

carbon monoxide consumption per mass of oxide, and the latter is directly proportional to the rate of the change in non-stoichiometry, as follows:

$$\dot{V}_{\mathrm{CO}}(t)=\frac{V_{\mathrm{M}}}{M_{\mathrm{CeO_2}}}\frac{\mathrm{d}\delta_{\mathrm{red}}}{\mathrm{d}t} \tag{6}$$

where V_{M} and $M_{\mathrm{CeO_2}}$ are the molar volume of O_2 and the molecular mass of the oxide, respectively. Moreover, for the convenience of calculation, the molar mass in the fully oxidized state is adopted.

2.3 Model of the oxidation step

In the oxidation reaction, oxides are oxidized again in an inert gas environment containing water, while water is split to produce hydrogen. The volume flow rate of inert gas is constant at F_{ox}, and the volume fraction containing water is $\chi_{\mathrm{H_2O}}$. Its reaction proceeds according to the following formula:

$$\frac{1}{\Delta\delta}\mathrm{CeO}_{2-\delta_{\mathrm{f}}}+\mathrm{H_2O}\rightarrow\frac{1}{\Delta\delta}\mathrm{CeO}_{2-\delta_{\mathrm{i}}}+\mathrm{H_2} \tag{7}$$

The rate of the change in oxygen vacancies over time in this process can be obtained by the mass balance of hydrogen and oxygen, as follows:

$$\frac{\mathrm{d}\delta_{\mathrm{ox}}}{\mathrm{d}t}=\frac{F_{\mathrm{ox}}}{n_{\mathrm{CeO_2}}}\times\frac{(2P_{\mathrm{O_2}}(\delta,T_0)-\psi_{\mathrm{H_2O}}\chi_{\mathrm{H_2O}}(P_{\mathrm{tot}}-P_{\mathrm{O_2}}(\delta,T_0)))}{(P_{\mathrm{tot}}-P_{\mathrm{O_2}}(\delta,T_0))} \tag{8}$$

where $\Delta\delta_{\mathrm{ox}}=-\Delta\delta_{\mathrm{red}}=\delta_{\mathrm{i}}-\delta_{\mathrm{f}}$, and $\psi_{\mathrm{H_2O}}$ is the proportion of H_2O that undergoes splitting. In addition to oxidation reaction (7), water also undergoes decomposition reaction at high temperatures, and the latter reaction is described as follows:

$$\mathrm{H_2O}\rightleftharpoons\frac{1}{2}\mathrm{O_2}+\mathrm{H_2} \tag{9}$$

$K_{\mathrm{H_2O},T_0}$ is used to indicate the degree of this reversible reaction, and it has a specific relationship with $\psi_{\mathrm{H_2O}}$:

$$K_{\mathrm{H_2O},T_0}=\frac{\psi_{\mathrm{H_2O}}}{(1-\psi_{\mathrm{H_2O}})}P_{\mathrm{O_2}}(\delta,T_0)^{\frac{1}{2}} \tag{10}$$

Similar to the calculation method for CO consumption, the direct changes in hydrogen production and oxygen non-stoichiometry are obtained:

$$\dot{V}_{\mathrm{H_2}}(t)=-\frac{V_{\mathrm{M}}}{2M_{\mathrm{CeO_2}}}\frac{\mathrm{d}\delta_{\mathrm{ox}}}{\mathrm{d}t} \tag{11}$$

The expressions for the oxidation process are similar to those in the process described by Haile et al., which is matched with the reduction process driven by CO in this work[21].

2.4 Thermodynamic evaluation

The solar energy to fuel conversion efficiency and the conversion rate of reactants are selected as key indicators for system evaluation. The solar energy to fuel conversion efficiency ($\eta_{\text{solar-to-fuel}}$) is defined as the ratio of the higher heating value of hydrogen produced to the input of solar energy:

$$\eta_{\text{solar-to-fuel}}=\frac{\dot{n}_{\mathrm{H_2}}HHV_{\mathrm{H_2}}}{Q_{\text{solar}}/\eta_{\text{abs}}} \tag{12}$$

in which $\dot{n}_{\mathrm{H_2}}$ and $HHV_{\mathrm{H_2}}$ are the flow rate of H_2 generation and the higher heating value of H_2 (285.83 kJ $\mathrm{mol^{-1}}$), respectively. Q_{solar} refers to the total solar energy input to the system, which includes three parts in the isothermal cycle: the energy used for reducing oxide (Q_{red}), the energy used for heating water ($Q_{\mathrm{H_2O}}$), and the energy used for heating carbon monoxide (Q_{CO}). Here, the heating process of gases that do not participate in the reaction, such as Ar and CO_2, is ignored. As follows:

$$Q_{\text{solar}}=Q_{\text{red}}+Q_{\mathrm{H_2O}}+Q_{\mathrm{CO}} \tag{13}$$

Q_{red} is given by

$$Q_{\text{red}}=\frac{1}{\delta_{\mathrm{f}}-\delta_{\mathrm{i}}}\int_{\delta_{\mathrm{i}}}^{\delta_{\mathrm{f}}}(-\Delta H_{\text{oxide}}(\delta))\,\mathrm{d}\delta \tag{14}$$

where $\Delta H_{\text{oxide}}(\delta)$ is the change in the molar thermal reduction enthalpy of the oxide. $Q_{\mathrm{H_2O}}$ and Q_{CO} are given by

$$Q_{\mathrm{H_2O}}=n_{\mathrm{H_2O,in}}\left(\int_{298\mathrm{K}}^{373\mathrm{K}}C_{p,\mathrm{H_2O(l)}}\mathrm{d}T+\Delta H_{\mathrm{H_2O(l)}\rightarrow\mathrm{(g)}}^{373\mathrm{K}}+\int_{373\mathrm{K}}^{T}C_{p,\mathrm{H_2O(g)}}\mathrm{d}T\right) \tag{15}$$

and

$$Q_{\mathrm{CO}}=n_{\mathrm{CO,in}}\int_{298\mathrm{K}}^{T}C_{p,\mathrm{CO}}\mathrm{d}T \tag{16}$$

where $n_{\mathrm{H_2O,in}}$ and $n_{\mathrm{CO,in}}$ are the molar amounts of water and carbon monoxide input into the system, respectively[23]. The absorption efficiency of solar energy η_{abs} is a function of both the reaction temperature T and concentration ratio C:

$$\eta_{abs} = 1 - \frac{\sigma T^4}{IC} \quad (17)$$

in which the solar irradiation I is 1000 W m^{-2} and the concentration ratio C is 5000.

The conversion rate of reactants is defined as the proportion of gases participating in the reaction to the total input, and the conversion rates of carbon monoxide and water are given by

$$X_{CO} = (n_{CO,in} - n_{CO,out})/n_{CO,in} \quad (18)$$

and

$$X_{H_2O} = (n_{H_2O,in} - n_{H_2O,out})/n_{H_2O,in} \quad (19)$$

where $n_{H_2O,out}$ and $n_{CO,out}$ are the molar amounts of H_2O and CO at the outlet, respectively.

3. RESULTS AND DISCUSSION

3.1 Upgrade of the oxygen non-stoichiometry

The changes in the oxygen non-stoichiometry of metal oxides during the isothermal cycle at 1500 °C are shown in Figure 3. The CO driven reduction reaction has a lower oxygen partial pressure compared to the strategy using inert sweeping gas, indicating a better deoxygenation effect. Moreover, for pure $CeO_{2-\delta}$ and $Ce_{0.80}Zr_{0.20}O_{2-\delta}$, the δ values in the CO driven cycle are 0.069-0.087 and 0.037-0.130, respectively, which are

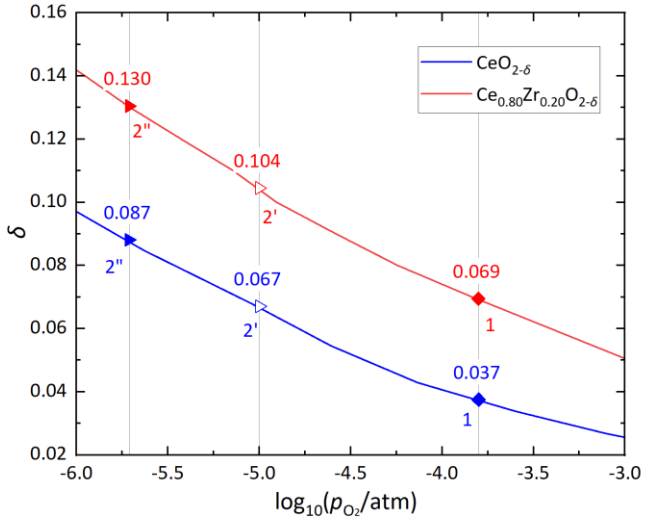

Fig. 3. The change in oxygen non-stoichiometry of metal oxides during an isothermal cycle at 1500 °C. The blue line represents pure ceria, while the red line represents ceria doped with 20% Zr^{4+} ($Ce_{0.80}Zr_{0.20}O_{2-\delta}$). State 1 indicates the δ value of the oxides at the end of the oxidation reaction, state 2' indicates the δ value after the reduction reaction using the inert sweeping gas strategy, and state 2'' indicates the δ value after the CO driven reduction reaction.

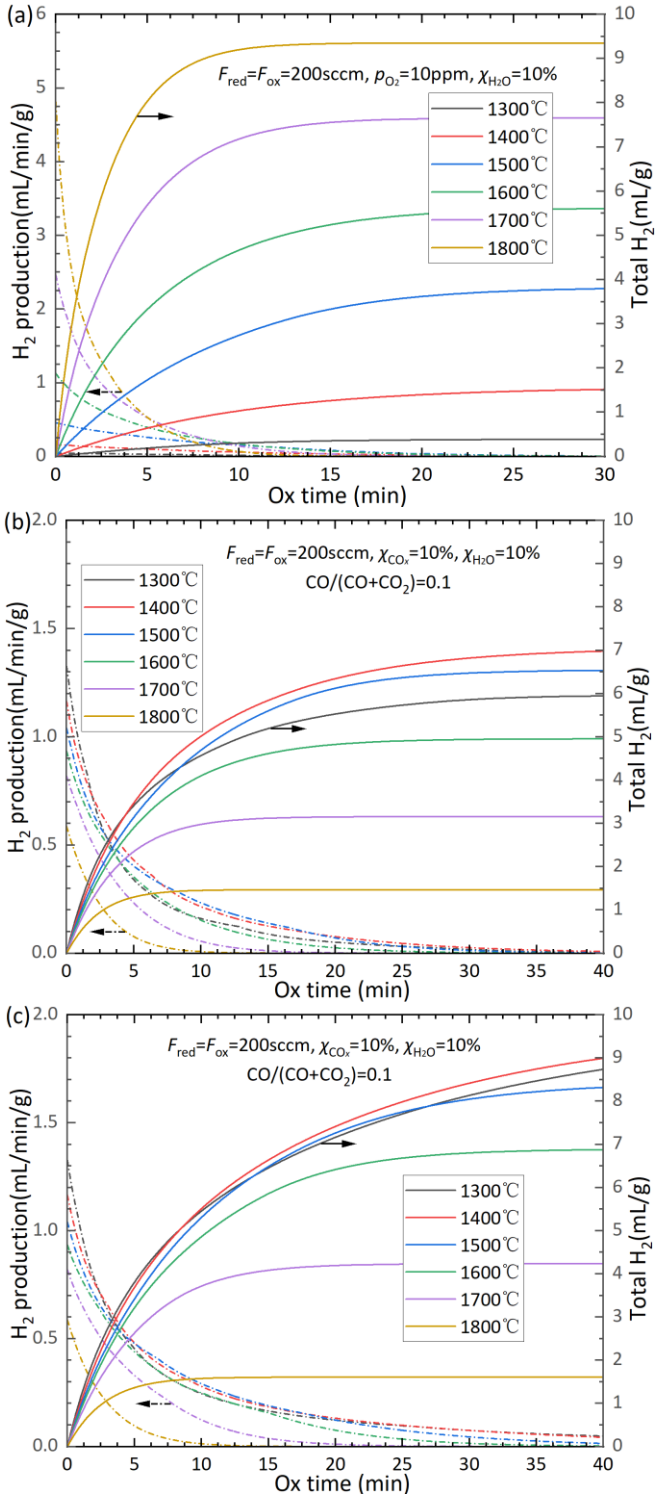

Fig. 4 The kinetic and thermodynamic performance of the solar thermochemical isothermal cycles using two different strategies. The inert sweeping gas strategy is adopted in (a), while the CO driven reduction reaction strategy is adopted in (b) and (c). Moreover, in (a) and (b), oxygen carriers are based on $CeO_{2-\delta}$, while they are based on $Ce_{0.80}Zr_{0.20}O_{2-\delta}$ in (c).

much greater than the values of 0.069-0.067 and 0.037-0.104, respectively, for the inert sweeping gas strategy.

3.2 Kinetic and thermodynamic performance

The kinetic and thermodynamic performance of the two oxides in solar thermochemical isothermal cycles using two different strategies is shown in Figure 4. The airflow conditions in the cycle using the same strategy are consistent, and the mass of oxides is 0.5 g.

The temperature setting range for the isothermal cycles is 1300-1800 °C. With increasing temperature, the CO driven cycle exhibits significantly different performance changes compared to the cycle using the inert sweeping gas strategy. Its hydrogen production rate and total amount both increase and then decrease with increasing temperature, and there is an optimal temperature of approximately 1400 °C.

The CO driven cycle has outstanding fuel production capacity at low or medium temperatures. If the total hydrogen production exceeds 6 mL/g, its cycle temperature is approximately 200-300 °C lower than that when using the inert sweeping gas strategy, which makes it more advantageous for reactor designing and matching with the solar concentration.

It is worth noting that the larger $\Delta\delta$ in the CO driven cycle leads to an extension of its oxidation reaction time, which will result in a longer supply of water during the oxidation process, requiring more energy to heat this water, and may ultimately lead to a decrease in cycle efficiency.

The reasons for the inhibition of CO driven cycle performance by high temperature are shown in Figure 5, which may be attributed to the increased reaction degree of equation (2) at high temperature limiting the elimination of O_2 in the reverse reaction.

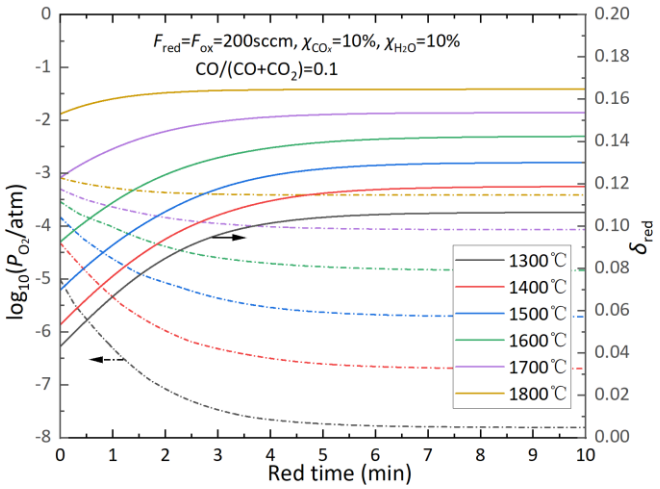

Fig. 5 The trend of δ and P_{O_2} over time during the CO driven reduction process of $Ce_{0.80}Zr_{0.20}O_{2-\delta}$.

3.3 Efficiency of the system

A stable cycle in continuous cycles is selected to evaluate the efficiency of the system and the conversion rate of the reactants, with the reduction reaction time of 10 minutes and oxidation reaction time of 15 minutes. A longer oxidation reaction time is disadvantageous, as $d\delta/dt$ is much smaller in the later stage of the reaction than in the earlier stage. Therefore, achieving higher efficiency by controlling the reaction time rather than yielding the maximum fuel production per unit of oxide over a longer period of time is cost-effective.

The effect of temperature on the conversion rate of reactants in isothermal cycles is shown in Figure 6. The conversion rate of water is less than 2% under all conditions, and the energy of heating water is an important source of irreversible loss. Therefore, in subsequent efficiency calculations, only high-temperature water is subjected to 95% heat recovery. At 1300-1500 °C, the CO conversion rate based on the two types of oxides is between 15-25%, and there is still a significant excess of CO.

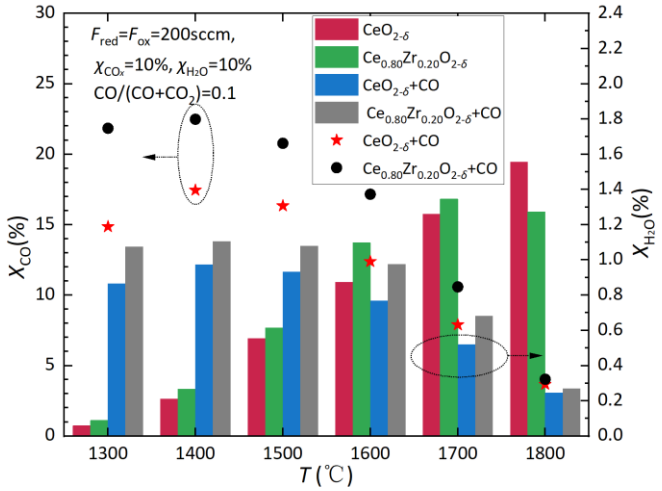

Fig. 6 The relationship between the conversion rate of reactants and the change in isothermal temperature.

Figure 7 demonstrates the influence of temperature and water heat recovery rate on the conversion efficiency of solar energy to fuel ($\eta_{\text{solar-to-fuel}}$). At 1300 °C, the $\eta_{\text{solar-to-fuel}}$ of the CO driven cycles reaches 19.89% and 23.77% with 95% water heat recovery when $CeO_{2-\delta}$ and $Ce_{0.80}Zr_{0.20}O_{2-\delta}$ are used as oxygen carriers, respectively. To achieve these $\eta_{\text{solar-to-fuel}}$, the reduction temperature should above 1600 °C in the traditional cycles of ceria using the inert sweeping gas strategy.

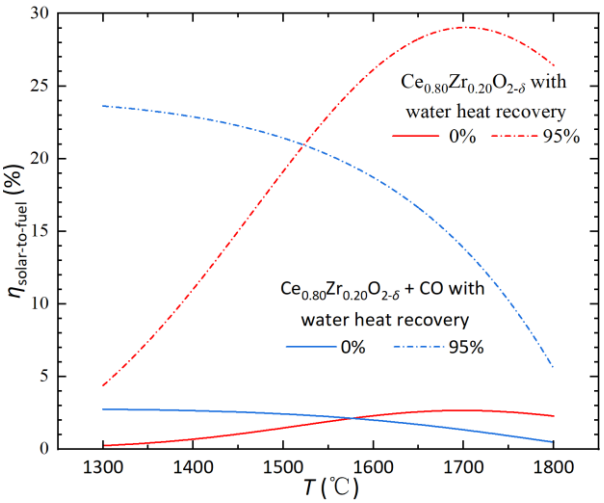

Fig. 7 The influence of temperature and heat recovery rate on the solar energy to fuel conversion efficiency.

4. CONCLUSIONS

In this research, a kinetic-thermodynamic model of an efficient solar thermochemical cycling system for hydrogen production driven by carbon monoxide is established. The introduction of carbon monoxide decreases the Gibbs free energy of the reduction reaction and removes oxygen from the reactor, achieving a coupled modification in cycle temperature and oxygen partial pressure. When $CeO_{2-\delta}$ and $Ce_{0.80}Zr_{0.20}O_{2-\delta}$ are selected as oxygen carriers, the theoretical solar energy to fuel conversion efficiencies of CO driven isothermal cycles at 1300 °C can reach 19.89% and 23.77%, respectively, with only water heat recovery.

This work provides rational guidance for the design of the solar thermochemical cycling system for hydrogen production. Further and in-depth research on the optimal reaction temperature and inlet gas composition for this cycle to improve system efficiency will be a key consideration in the future.

ACKNOWLEDGEMENT

This work was funded by the National Natural Science Foundation of China (No. 52006124), the Beijing Natural Science Foundation (No. 3232031), the National Key R&D Program of China (Grant No. 2023YFE0113000), the GuangDong Basic and Applied Basic Research Foundation (No. 2023A1515240008) and the Young Elite Scientists Sponsorship Program by CAST (No. 2023QNRC001).

REFERENCES

[1] Bayon A, de la Calle A, Ghose KK. Experimental, computational and thermodynamic studies in perovskites metal oxides for thermochemical fuel production: A review. International Journal of Hydrogen Energy 2020;45(23):12653-12679. Doi:10.1016/j.ijhydene.2020.02.126.

[2] Safari F, & Dincer I. A review and comparative evaluation of thermochemical water splitting cycles for hydrogen production. Energy Conversion and Management 2020;205. Doi:10.1016/j.enconman.2019.112182.

[3] Kim J, Henao CA, Johnson TA. Methanol production from CO_2 using solar-thermal energy: process development and techno-economic analysis. Energy & Environmental Science 2011;4(9). Doi:10.1039/c1ee01311d.

[4] Rytter E, Soušková K, Lundgren MK. Process concepts to produce syngas for Fischer-Tropsch fuels by solar thermochemical splitting of water and/or CO_2. Fuel Processing Technology 2016;145:1-8. Doi:10.1016/j.fuproc.2016.01.015.

[5] Guo Y, Chen J, Song H. A review of solar thermochemical cycles for fuel production. Applied Energy 2024;357. Doi:10.1016/j.apenergy.2023.122499.

[6] Chueh WC, Falter C, Abbott M. High-flux solar-driven thermochemical dissociation of CO_2 and H_2O using nonstoichiometric ceria. Science 2010;330(6012):1797-1801. Doi:10.1126/science.1197834.

[7] Chen J, Kong H, & Wang H. A novel high-efficiency solar thermochemical cycle for fuel production based on chemical-looping cycle oxygen removal. Applied Energy 2023;343. Doi:10.1016/j.apenergy.2023.121161.

[8] Marxer D, Furler P, Takacs M. Solar thermochemical splitting of CO_2 into separate streams of CO and O_2 with high selectivity, stability, conversion, and efficiency. Energy & Environmental Science 2017;10(5):1142-1149. Doi:10.1039/c6ee03776c.

[9] Ruan C, Huang Z-Q, Lin J. Synergy of the catalytic activation on Ni and the CeO_2-TiO_2/$Ce_2Ti_2O_7$ stoichiometric redox cycle for dramatically enhanced solar fuel production. Energy & Environmental Science 2019;12(2):767-779. Doi:10.1039/c8ee03069c.

[10] Bu C, Gu T, Cen S. Reactivity and stability of Zr-doped CeO_2 for solar thermochemical H_2O splitting in combination with partial oxidation of methane via isothermal cycles. International Journal of Hydrogen Energy 2023;48(33):12227-12239. Doi:10.1016/j.ijhydene.2022.11.232.

[11] Fosheim JR, Hathaway BJ, & Davidson JH. High efficiency solar chemical-looping methane reforming with ceria in a fixed-bed reactor. Energy 2019;169:597-612. Doi:10.1016/j.energy.2018.12.037.

[12] Jin F, Xu C, Xing J. Thermodynamic analysis of titanium dioxide-based isothermal methanothermal and

carbothermal redox cycles for solar fuel production. Energy Conversion and Management 2022;254. Doi:10.1016/j.enconman.2022.115254.
[13] Levêque G, & Abanades S. Investigation of thermal and carbothermal reduction of volatile oxides (ZnO, SnO_2, GeO_2, and MgO) via solar-driven vacuum thermogravimetry for thermochemical production of solar fuels. Thermochimica Acta 2015;605:86-94. Doi:10.1016/j.tca.2015.02.015.
[14] Guene Lougou B, Shuai Y, Chaffa G. Analysis of two‐step solar thermochemical looping reforming of Fe_3O_4 redox cycles for synthesis gas production. Energy Technology 2019;7(3). Doi:10.1002/ente.201800588.
[15] Kang K-S, Kim C-H, Bae K-K. Redox cycling of $CuFe_2O_4$ supported on ZrO_2 and CeO_2 for two-step methane reforming/water splitting. International Journal of Hydrogen Energy 2010;35(2):568-576. Doi:10.1016/j.ijhydene.2009.10.099.
[16] Kang K-S, Kim C-H, Cho W-C. Reduction characteristics of $CuFe_2O_4$ and Fe_3O_4 by methane; $CuFe_2O_4$ as an oxidant for two-step thermochemical methane reforming. International Journal of Hydrogen Energy 2008;33(17):4560-4568. Doi:10.1016/j.ijhydene.2008.05.054.
[17] Hou SS, Chen CH, Chang CY. Firing blast furnace gas without support fuel in steel mill boilers. Energy Conversion and Management 2011;52(7):2758-2767. Doi:10.1016/j.enconman.2011.02.009.
[18] Muhich CL, Evanko BW, Weston KC. Efficient Generation of H_2 by Splitting Water with an Isothermal Redox Cycle. Science 2013;341(6145):540-542. Doi:10.1126/science.1239454.
[19] Hao Y, Yang C-K, & Haile SM. Ceria-zirconia solid solutions ($Ce_{1-x}Zr_xO_{2-\delta}$, $x \leqslant 0.2$) for solar thermochemical water splitting: a thermodynamic study. Chemistry of Materials 2014;26(20):6073-6082. Doi:10.1021/cm503131p.
[20] Li K, Wang H, Wei Y. Partial oxidation of methane to syngas with air by lattice oxygen transfer over ZrO_2-modified Ce-Fe mixed oxides. Chemical Engineering Journal 2011;173(2):574-582. Doi:10.1016/j.cej.2011.08.006.
[21] Davenport TC, Yang C-K, Kucharczyk CJ. Maximizing fuel production rates in isothermal solar thermochemical fuel production. Applied Energy 2016;183:1098-1111. Doi:10.1016/j.apenergy.2016.09.012.
[22] Davenport TC, Yang CK, Kucharczyk CJ. Implications of exceptional material kinetics on thermochemical fuel production rates. Energy Technology 2016;4(6):764-770. Doi:10.1002/ente.201500506.
[23] Kong H, Hao Y, & Jin H. Isothermal versus two-temperature solar thermochemical fuel synthesis: A comparative study. Applied Energy 2018;228:301-308. Doi:10.1016/j.apenergy.2018.05.099.